Reanalysis of the $\beta - \bar{\nu}_e$ Angular Correlation Measurement from the aSPECT Experiment with New Constraints on Fierz Interference

M. Beck,[1] W. Heil,[1,*] Ch. Schmidt,[1] S. Baeßler,[2] F. Glück,[3] G. Konrad,[4] and U. Schmidt[5]

[1]*Institut für Physik, Johannes Gutenberg-Universität, 55128 Mainz, Germany*
[2]*Department of Physics, University of Virginia, Charlottesville, Virginia 22904, USA*
and Oak Ridge National Lab, Bethel Valley Road, Oak Ridge, Tennessee 37831, USA
[3]*Institut für Astroteilchenphysik (IAP), Karlsruhe Institute of Technology (KIT), 76344 Eggenstein-Leopoldshafen, Germany*
[4]*Technische Universität Wien, Atominstitut, 1020 Wien, Austria*
[5]*Physikalisches Institut, Ruprecht-Karls-Universität, 69120 Heidelberg, Germany*

On the basis of revisions of some of the systematic errors, we reanalyzed the electron-antineutrino angular correlation (a coefficient) in free neutron decay inferred from the recoil energy spectrum of the protons which are detected in 4π by the aSPECT spectrometer. With $a = -0.104\,02(82)$ the new value differs only marginally from the one published in 2020. The experiment also has sensitivity to b, the Fierz interference term. From a correlated (b, a) fit to the proton recoil spectrum, we derive a limit of $b = -0.0098(193)$ which translates into a somewhat improved 90% confidence interval region of $-0.041 \leq b \leq 0.022$ on this hypothetical term. Tighter constraints on b can be set from a combined [shown as superscript (c)] analysis of the PERKEO III (β asymmetry) and aSPECT measurement which suggests a finite value of b with $b^{(c)} = -0.0181 \pm 0.0065$ deviating by 2.82σ from the standard model.

Introduction.—The free neutron presents a unique system to investigate the standard model (SM) of particle physics. While the neutron lifetime gives the overall strength of the weak semileptonic decay, neutron decay correlation coefficients depend on the ratio of the coupling constants involved, and hence determine the internal structure of this decay. The aSPECT experiment [1–3] has the goal to determine the ratio of the weak axial-vector and vector coupling constants $\lambda = g_A/g_V$ from a measurement of the β–$\overline{\nu}_e$ angular correlation in neutron decay. The β-decay rate when observing only the electron and neutrino momenta and the neutron spin and neglecting a T-violating term is given by [4]

$$d^3\Gamma = G_F^2 V_{ud}^2 \left(1 + 3\lambda^2\right) p_e E_e (E_0 - E_e)^2$$
$$\times \left(1 + a\frac{\overrightarrow{p_e} \cdot \overrightarrow{p_\nu}}{E_e E_\nu} + b\frac{m_e}{E_e} + \frac{\overrightarrow{\sigma_n}}{\sigma_n} \cdot \left[A\frac{\overrightarrow{p_e}}{E_e} + B\frac{\overrightarrow{p_\nu}}{E_\nu}\right]\right)$$
$$\times dE_e d\Omega_e d\Omega_\nu \tag{1}$$

with $\overrightarrow{p_e}$, $\overrightarrow{p_\nu}$, E_e, E_ν being the momenta and total energies of the beta electron and the electron-antineutrino, m_e the mass of the electron, G_F the Fermi constant, V_{ud} the first element of the Cabbibo-Kobayashi-Maskawa (CKM) matrix, E_0 the total energy available in the transition, and $\overrightarrow{\sigma_n}$ the spin of the neutron. The quantity b is the Fierz interference coefficient. It vanishes in the purely vector axial-vector (V-A) interaction of the SM since it requires left-handed scalar (S) and tensor (T) interactions (see below). The correlation coefficients a and A (β-asymmetry parameter [5,6]) are most sensitive to λ and are used for its determination. The SM dependence of the electron-antineutrino angular correlation coefficient a on λ is given by [4,7,8]

$$a = \frac{1 - |\lambda|^2}{1 + 3|\lambda|^2}. \tag{2}$$

In short, at aSPECT the a coefficient is inferred from the energy spectrum of the recoiling protons from the β decay of free neutrons. The shape of this spectrum is sensitive to a and it is measured in 4π by the aSPECT spectrometer using magnetic adiabatic collimation with an electrostatic filter (MAC-E filter) [9,10]. This technique in general offers a high luminosity combined with a well-defined energy resolution at the same time. In order to extract a reliable value of a, any effect that changes the shape of the proton energy spectrum, or to be more specific—the integral of the product of the recoil energy spectrum and the spectrometer transmission function—has to be understood and quantified precisely. With the analysis of all known sources of systematic errors at that time and their inclusion in the final result by means of a global fit, the aSPECT Collaboration published the value $a = -0.10430(84)$ [11]. From this, the ratio of axial-vector to vector coupling constants was derived giving $|\lambda| = 1.2677(28)$. This value deviates by $\approx 3\sigma$ from the most precise PERKEO III result [5],

determined via the β-asymmetry parameter A. One possible explanation for this discrepancy are hypothetical scalar or tensor couplings in addition to the V-A interaction of the SM. In this case, the overall decay probability may be modified by the Fierz interference term b according to Eq. (1) which would also change the measured values of many of the correlation coefficients; see also Refs. [12,13]. On the other hand, SM differences might be of experimental origin, which generally requires a critical reexamination of the systematics in the respective datasets. Consequently, the aSPECT data were reanalyzed as it could not be ruled out that previously overlooked systematics in (i) backscattering and below threshold losses in the detector and (ii) the retardation voltage U_{AP} of the electrostatic filter could be the reason for the discrepancies in the λ values. With these revised systematics included in the global data fit, a new SM analysis of the correlation parameter a is performed as well as a combined (a, b) analysis in order to put a direct constraint on the Fierz interference term from a single measurement. Tighter constraints on b can be set by using the PERKEO III data, where limits on b have been derived via a combined (b, A) fit to their data.

Backscattering and below threshold losses.—Whereas the amount of electron-hole pair production in amorphous solids by a penetrating proton can be determined rather accurately with the binary collision code TRIM [14] (used in [11]), the calculation of the ionization depth profile in crystalline solids is more complicated due to channeling effects that TRIM does not attempt to take into account. In our reanalysis we simulated the slowing down of protons in our silicon drift detector (SDD) (processed on a $\langle 100 \rangle$-oriented Si wafer) by the program Crystal-TRIM originally developed in order to describe ion implantation into crystalline solids with several amorphous overlayers [15,16] (in our case: a 30 nm thick aluminum overlayer including its 4 nm thick alumina layer [17] on top). The range of applicability of this code was studied by comparing with existing molecular dynamics simulations. [18] With Crystal-TRIM good agreement (5%) was obtained for the parameter $C_{el} = 0.65$ in the semiempirical formula for the local electronic energy loss [16].

Together with the charge collection efficiency for this type of detector [20] at depth z and further taking into account charge exchange reactions of backscattered protons at the topmost detector layer (not considered so far) [21], we derive our simulated pulse height spectra. The latter ones are in excellent agreement with the experimental pulse height spectra at different acceleration voltages U_{acc} and retardation voltages U_{AP}. This procedure allows us to calculate the below-threshold losses including the events with no energy deposition inside the detector. For more details see [22]. Figure 1 shows the fractional losses for the two detector pads. In both cases a cubic spline interpolation was used to describe their retardation voltage dependence. In total, channeling and the inclusion of charge exchange
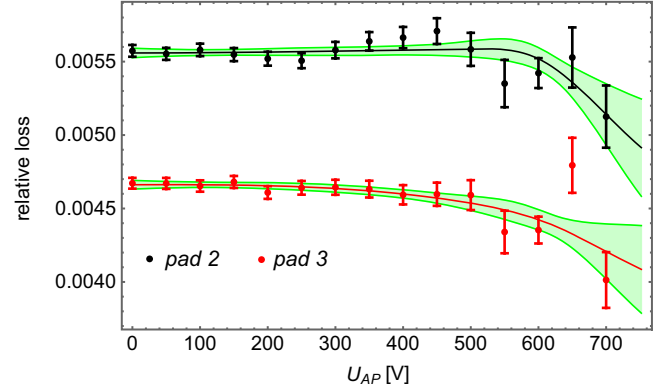

FIG. 1. Simulated fraction of undetected protons (both for pad 2 and pad 3 of the SDD) of the integral proton spectrum whose corresponding pulse heights fall below the threshold of the data acquisition system. The U_{AP} dependence of the simulated losses can be described by a cubic spline function (solid line) and is shown together with the 1σ error predicted by the global fit (green band).

reactions do not significantly influence the spectral shape of the undetected protons, as seen by comparison with Fig. 22 in [11]. The obvious higher fractional losses of $\approx 35\%$ (shape independent), which can be attributed to the equilibrium charge ratio of backscattered protons from the alumina layer, have no effect on the final result due to normalization (N_0).

Effective retardation voltage $\langle U_A \rangle$.—Like the magnetic field ratio $r_B = B_A/B_0$, where B_0 and B_A are the respective magnetic fields at the place of emission and retardation, the retardation voltage U_{AP} directly enters the spectrometer's adiabatic transmission function [2,31] given by

$$F_{tr}(T, U_{AP}, r_B)$$
$$= \begin{cases} 0 & \text{if } T \leq eU_{AP} \\ 1 - \sqrt{1 - \frac{T - eU_{AP}}{r_B T}} & \text{if } eU_{AP} < T < \frac{eU_{AP}}{1 - r_B}, \\ 1 & \text{if } T > \frac{eU_{AP}}{1 - r_B} \end{cases} \quad (3)$$

where T is the kinetic energy of the isotropically emitted protons. The inhomogeneities of the potential in the decay volume (DV) and the analyzing plane (AP) region result in a slight shift (determined from particle tracking simulation) of the effective retardation voltage $\langle U_A \rangle$ from the applied voltage U_{AP} due to spatial and temporal variations of the work function of the DV and AP electrodes. This shift and its functional dependence on U_{AP} is described in detail in [11]. A further source of uncertainty is the measurement precision $\sigma_{AP}^{\text{Agilent}}$ of the applied voltage by means of the Agilent 3458A multimeter. In the previous analysis this uncertainty was not correctly incorporated in the fit function as an error of the horizontal axis in the U_{AP} dependence of the integral proton spectrum. Instead, it was treated as part of an offset error $c_{\text{offset}}^{\langle U_A \rangle}$ common to all $\langle U_A \rangle$

TABLE I. Global fit results [at 68.27% convidence level (CL)] on a assuming the SM vector and axial-vector couplings only, together with an analysis allowing nonzero scalar or tensor interactions in order to derive limits on b. The error bars on a and b were scaled with $\sqrt{\chi^2/\nu}$ whenever the condition $p = \int_{\chi^2/\nu}^{\infty} f_\nu(\chi^2) d\chi^2 < 0.05$ was met with $f_\nu(\chi^2)$ being the χ^2-distribution function with ν degrees of freedom [39].

	a	Δa	b	Δb	χ^2/ν	p-value
Results from [11]	$-0.104\,30$	$0.000\,84$	$\cdots$	$\cdots$	$1.440 (\nu = 268)$	3.1×10^{-6}
Reanalysis	$-0.104\,02$	$0.000\,82$	$\cdots$	$\cdots$	$1.245 (\nu = 264)$	4.1×10^{-3}
(a, b) analysis	$-0.104\,59$	$0.001\,39$	-0.0098	0.0193	$1.249 (\nu = 263)$	3.7×10^{-3}

values. We now improve our analysis by replacing Eq. (3) through

$$F_{\mathrm{tr}}(T, U_{\mathrm{AP}}, r_{\mathrm{B}}) \to F_{\mathrm{tr}}(T, \langle U_{\mathrm{A}} \rangle, r_{\mathrm{B}}) + \frac{\partial F_{\mathrm{tr}}}{\partial U_{\mathrm{AP}}} \Delta U_{\mathrm{AP}}^{\mathrm{Agilent}}. \quad (4)$$

Here, $\sigma_{\mathrm{AP}}^{\mathrm{Agilent}}$ enters the transmission function via the partial derivative $\Delta F_{\mathrm{tr}}^{\mathrm{Agilent}} = (\partial F_{\mathrm{tr}}/\partial U_{\mathrm{AP}}) \Delta U_{\mathrm{AP}}^{\mathrm{Agilent}}$. In the fit procedure, $\Delta U_{\mathrm{AP}}^{\mathrm{Agilent}}$ is a restricted fit parameter, Gaussian distributed with zero mean and $\sigma_{\mathrm{AP}}^{\mathrm{Agilent}} = 13$ mV.

Global fit results.—In the ideal case without any systematic effect, the fit to the proton integral count rate spectrum would be a χ^2 minimization of the fit function

$$f_{\mathrm{fit}}(U_{\mathrm{AP}}, r_{\mathrm{B}}; a, N_0) = N_0 \int_0^{T_{\max}} \omega_{\mathrm{p}}(T, a) F_{\mathrm{tr}}(T, U_{\mathrm{AP}}, r_{\mathrm{B}}) dT \quad (5)$$

with the overall prefactor N_0 and a as free fit parameters. The way to include all systematic corrections to the global fit, the reader is advised to refer to the relevant Sec. III C of [11] for details. The theoretical proton recoil spectrum $\omega_{\mathrm{p}}(T, a)$ is given by Eqs. (3.11) and (3.12) in [32] with λ replaced by a [Eq. (2)]. This spectrum includes relativistic recoil and higher order Coulomb corrections, as well as order-α radiative corrections [32–34]. For the precise computation of the $F(Z = 1, E_e)$ Fermi function (Coulomb corrections), we have used formula (ii) in Appendix 7 of Ref. [35]. The weak magnetism $\kappa = (\mu_p - \mu_n)/2$ (conserved vector current value) is included in the (E_p, E_e) Dalitz distribution, but essentially drops out in the proton-energy spectrum after integration over the electron energy E_e [36]. All corrections taken together are precise to a level of $\Delta a/a \approx 0.1\%$.

The aSPECT experiment also has sensitivity to b, the Fierz interference term [see Eq. (1)]. The $1/E_e$ dependency results in small deviations from the SM proton recoil spectrum. In Eqs. (4.10) and (4.11) of [37] an analytical expression of $\omega_{\mathrm{p}}^*(T, a)$ is given where recoil-order effects and radiative corrections are neglected [38]. To add the b term to the complete spectrum $\omega_{\mathrm{p}}(T, a)$, we define $\omega_{\mathrm{p}}(T, a, b)$ by adding an additional term $4/(1 + 3a) m_e E_e (E_{2\mathrm{m}} - E_e/2) \cdot b$ to the right-hand side of

Eq. (3.12) in [32], and replace $\Delta = m_n - m_p$ by $E_{2\mathrm{m}} = \Delta - (\Delta^2 - m_e^2)/(2m_n)$. For the final result, we performed a global fit as described in Sec. V of [11]. Table I summarizes the results on a from the purely SM approach, i.e., $\omega_{\mathrm{p}}(T, a)$ as well as the simultaneous (b, a) fit results if the proton recoil spectrum $\omega_{\mathrm{p}}(T, a, b)$ would be modified by the Fierz interference term b.

The error on a from the respective fit is the total error scaled with $\sqrt{\chi^2/\nu}$. Besides the statistical error, it contains the uncertainties of the systematic corrections and the correlations among the fit parameters which enter the variance-covariance matrix to calculate the error on the derived quantity from the fit. In [11] we stated that the elevated χ^2/ν values of the global-a fit most likely arise due to the nonwhite reactor power noise and/or high-voltage induced background fluctuations (cf. Sec. IV A there). The reanalysis of the aSPECT data now leads to a reduced $\chi^2/\nu = 1.25$ ($p = 4.1 \times 10^{-3}$ for $\nu = 264$). The revision of the U_{AP} error is the main driver for this and for the corresponding changes to a.

Our new value for the a coefficient only differs marginally from the one published in [11] (see Table I) and is given by

$$a = -0.104\,02 \pm 0.000\,82. \quad (6)$$

Using Eq. (2) we derive for λ the value $\lambda = -1.2668(27)$.

If one allows for b as a free parameter, we obtain from the measurement of the proton recoil spectrum a limit at 68.27% CL for the Fierz interference term of

$$b = -0.0098 \pm 0.0193. \quad (7)$$

In the combined fit, the error on a increases by a factor of 1.7 as compared to the SM analysis with $b \equiv 0$ (Table I), since the two fit parameters show a fairly strong correlation: the off-diagonal element $\rho_{a,b}$ of the correlation matrix is $\rho_{a,b} = 0.808$ as a result of the global fit. Our limit can be rewritten as $-0.041 \le b \le 0.022$ (90% CL) which is currently the most precise one from neutron β decay [40].

Combined analysis of recent measurements of PERKEO III and aSPECT.—Further constraints on b can be set by using the PERKEO III data, where comparable limits on b have been derived from the measurement of the β asymmetry
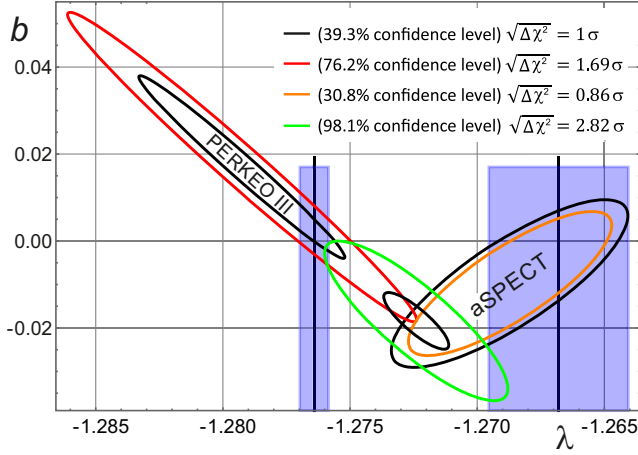
FIG. 2. Confidence region for the ratio $\lambda = g_A/g_V$ and the Fierz interference parameter b. The results of a correlated (b, λ) analysis of the PERKEO III and aSPECT measurements are shown as error ellipses representing specified confidence levels. The combined [shown as superscript (c)] result from the two independent datasets suggests a finite value of b with $b^{(c)} = -0.0181(65)$ which deviates by 2.82σ from the SM (shown by the green error ellipse). The 90% CL interval of $-0.012 < b < +0.144$ from UCNA [43] is consistent with $b^{(c)}$ or a vanishing b value. For the SM analysis ($b \equiv 0$) of the two measurements, the λ values of PERKEO III and aSPECT disagree by 3.4 standard deviations (blue vertical bars: 1σ error).

in neutron decay via a combined (b, A) fit to their data (see Fig. 3 in [41]). Including other measurements like UCNA [42,43], aCORN [44,45], and PERKEO II [46] would not add substantial information. Besides, error ellipse data (see Fig. 2) are not (or not yet) published. To allow a direct comparison, the neutron decay parameters A and a are expressed in terms of λ (see e.g., [8]). Figure 2 shows the error ellipses in the (b, λ) plane which represent the iso-contours of the respective bivariate Gaussian probability distributions (PDF) to visualize a 2D confidence interval [47]. Both experiments on their own show a value of b compatible with zero in the 1σ range of their error ellipses ($p_{cl} = 39.35\%$). With $\rho_{A,b} = -0.985$, the PERKEO III ellipses have a very strong negative correlation and are almost orthogonal to the ones from the aSPECT (b, a) analysis. This orthogonality, in turn, leads to a stronger constraint in b as can be seen directly from the overlap of error ellipses their assigned confidence levels (p_{cl}) are beyond $p_{cl} > 40\%$. From the combined error ellipse, which represents the iso-contour of the product of the respective PDFs, we can deduce that the case $b = 0$ lies on the edge of its 98.1% confidence region. The resulting values for (b, λ) at 68% CL in combining [shown as superscript (c)] the independent datasets of PERKEO III and aSPECT are

$$b^{(c)} = -0.0181 \pm 0.0065,$$
$$\lambda^{(c)} = -1.2724 \pm 0.0013. \tag{8}$$

With 2.82σ, the Fierz interference term $b^{(c)}$ obtained deviates from zero while $\lambda^{(c)}$ lies in between the derived PERKEO III and aSPECT values for λ from the prior SM analysis [5,11]. Note that the most accurate results for A and a differ in their derived λ values by 3.4 standard deviations within the SM approach (see Fig. 2).

In order to check that the PERKEO III (P) and aSPECT (A) measurements of (b, λ) are statistically compatible with the combined result given in Eq. (8), we used the generalized least squares method [48] for fitting. Taking the 4×4 covariance matrix

$$\Omega = \begin{pmatrix} \Sigma(P) & 0 \\ 0 & \Sigma(A) \end{pmatrix} \tag{9}$$

and the 4-vector $V^T = (b^{(P)} - b^{(c)}, \lambda^{(P)} - \lambda^{(c)}, b^{(A)} - b^{(c)}, \lambda^{(A)} - \lambda^{(c)})$, $\chi^2 = V^T \Omega^{-1} V$ was minimized with $b^{(c)}$ and $\lambda^{(c)}$ as free parameters ($\nu = 2$). As input, we took the known quantities $b^{(P)}, \lambda^{(P)}, \Sigma(P)$ and $b^{(A)}, \lambda^{(A)}, \Sigma(A)$ from the respective measurements with Σ denoting the 2×2 variance-covariance matrix. With $\chi^2_{\nu=2} = 3.6$ (goodness of fit test), we arrive at the same results as in Eq. (8). The resulting p-value is $p = 0.16$ and is above the threshold of significance (typically 0.05 [39]). In Fig. 2, the error ellipses with the respective confidence level $p_{cl}(A) = 0.31$ and $p_{cl}(P) = 0.76$ are drawn which both touch in the center of the combined error ellipse. The p-value of 0.16 is reproduced by taking the product $[1 - p_{cl}(A)] \cdot [1 - p_{cl}(P)]$ [49].

The nonzero value of the Fierz interference term $b^{(c)}$ in neutron β decay is in tension with constraints from low energy precision β-decay measurements (pion [50–52], neutron, and nuclei [53,54]) as well as Large Hadron Collider (LHC) constraints through the reaction $pp \to e\nu + X$ and $pp \to e^+ e^- + X$ [55]. The $b^{(c)}$ and $\lambda^{(c)}$ values of Eq. (8) predict the neutron lifetime value of $\tau_n^{(c)} = (894.2 \pm 4.2)$ s using the master formula from [56,57] multiplied by the factor $(1 + \langle m_e/E_e \rangle \cdot b)^{-1}$ [58] on the right-hand side. This differs by 3.7σ from the PDG value for the neutron lifetime $\tau_n = (878.4 \pm 0.5)$ s [40].

As shown by Falkowski et al. [53], the SM difference could also be attributed to right-handed couplings for tensor currents ($C_T = -C'_T$ and $b_{Fierz} = 0$). By taking the PDG values for the neutron lifetime and the decay parameters A and B [40], including our result on a [Eq. (6)], a $(\lambda, |C_T/C_A|)$ fit to the data expressed in terms of the Lee-Yang Wilson coefficients [53] shows a striking preference for a nonzero value of the beyond-SM parameter $|C_T/C_A|$ with $|C_T/C_A| = 0.047 \pm 0.018$. While this result lies within the recent low energy limits $|C_T/C_A| < 0.087$ (95.5% CL) of [59], the LHC bounds $|C_T/C_A| = 4g_T|\tilde{\epsilon}_T/g_A| < 1.3 \times 10^{-3}$ from $pp \to e\nu + X$ [55,60] are more stringent than those from β decays.

Conclusion and Outlook.—In this Letter, we presented a reanalysis of the aSPECT data with an improved tracking of some of the systematic errors. The value $a = -0.104\,02(82)$ differs only marginally from the one published in [11]. The aSPECT experiment has sensitivity to b. We extract a limit of $b = -0.0098(193)$ on the Fierz interference term from a combined (b, a) analysis of the proton recoil spectrum. The apparent tension to the PERKEO III result [5] based on the SM analysis can be resolved by combining the results of the (b, λ) analyses from these two measurements. The finite value for the Fierz interference term of $b^{(c)} = -0.0181(65)$ deviates by 2.82σ from the SM. The goodness of fit test shows that the (b, λ) data from PERKEO III and aSPECT are statistically compatible with the combined result. The upcoming Nab experiment [61] and the next generation instruments like PERC [62,63] will allow the measurement of decay correlations with strongly improved statistical uncertainties to underpin these findings or to establish that the SM differences are of experimental origin.

———————

*Corresponding author: wheil@uni-mainz.de

[1] S. Baeßler, F. Ayala Guardia, M. Borg, F. Glück, W. Heil, G. Konrad, I. Konorov, R. Muñoz Horta, G. Petzoldt, D. Rich *et al.*, Eur. Phys. J. A **38**, 17 (2008).

[2] F. Glück, S. Baeßler, J. Byrne, M. G. D. van der Grinten, F. J. Hartmann, W. Heil, I. Konorov, G. Petzoldt, Y. Sobolev, and O. Zimmer, Eur. Phys. J. A **23**, 135 (2005).

[3] O. Zimmer, J. Byrne, M. van der Grinten, W. Heil, and F. Glück, Nucl. Instrum. Methods Phys. Res., Sect. A **440**, 548 (2000).

[4] J. Jackson, S. Treiman, and H. Wyld, Phys. Rev. **106**, 517 (1957).

[5] B. Märkisch *et al.* (PERKEO III Collaboration), Phys. Rev. Lett. **122**, 242501 (2019).

[6] M.-P. Brown *et al.* (UCNA Collaboration), Phys. Rev. C **97**, 035505 (2018).

[7] M. Fierz, Z. Phys. **104**, 553 (1937).

[8] H. Abele, Prog. Part. Nucl. Phys. **60**, 1 (2008).

[9] V. Lobashev and P. Spivak, Nucl. Instrum. Methods Phys. Res., Sect. A **240**, 305 (1985).

[10] A. Picard *et al.*, Nucl. Instrum. Methods Phys. Res., Sect. B **63**, 345 (1992).

[11] M. Beck *et al.* (aSPECT Collaboration), Phys. Rev. C **101**, 055506 (2020).

[12] M. González-Alonso and O. Naviliat-Cuncic, Phys. Rev. C **94**, 035503 (2016).

[13] M. González-Alonso, O. Naviliat-Cuncic, and N. Severijns, Prog. Part. Nucl. Phys. **104**, 165 (2019).

[14] J. F. Ziegler, M. Ziegler, and J. Biersack, Nucl. Instrum. Methods Phys. Res., Sect. A **268**, 1818 (2010).

[15] M. Posselt and J. P. Biersack, Nucl. Instrum. Methods Phys. Res., Sect. B **64**, 706 (1992).

[16] M. Posselt, Radiat. Effects Def. Solids **130/131**, 87 (1994).

[17] P. Dumas, J. P. Dubarry-Barbe, D. Riviere, Y. Levy, and J. Corset, J. Phys. (Paris), Colloq. **44**, C10-205 (1983).

[18] Molecular dynamics (MD) methods are well suited to study ion penetration in materials at energies where also multiple simultaneous collisions may be significant. The MDRANGE code [19], however, requires too extensive computation time given the high number of particle tracking simulations ($\approx 2 \times 10^7$ protons).

[19] K. Nordlund, Comput. Mater. Sci. **3**, 448 (1995).

[20] M. Popp, R. Hartmann, H. Soltau, L. Strüder, N. Meidinger, P. Holl, N. Krause, and C. von Zanthier, Nucl. Instrum. Methods Phys. Res., Sect. A **439**, 567 (2000).

[21] J. A. Phillips, Phys. Rev. **97**, 404 (1955).

[22] See Supplemental Material, which includes Refs. [23–30], at http://link.aps.org/supplemental/10.1103/PhysRevLett.132.102501 for more information on backscattering and below threshold losses.

[23] M. Simson, Ph.D. thesis, Technische Universität München, 2010.

[24] M. Simson, P. Holl, A. Miller, A. Niculae, G. Petzoldt, K. Schreckenbach, H. Soltau, L. Strüder, H.-F. Wirth, and O. Zimmer, Nucl. Instrum. Methods Phys. Res., Sect. A **581**, 772 (2007).

[25] H. Grahmann, A. Feuerstein, and S. Kalbitzer, Radiat. Eff. **29**, 117 (1976).

[26] K. Nordlund, F. Djurabekova, and G. Hobler, Phys. Rev. B **94**, 214109 (2016).

[27] M. Posselt, Crystal-TRIM Manual (2004), https://www.hzdr.de/db/Cms?pOid=66817.

[28] W. Khalid, Ph.D. thesis, Technische Universität Wien, 2023.

[29] G. Hobler, Radiat. Effects Def. Solids **139**, 21 (1996).

[30] P. Lechner, A. Pahlke, and H. Soltau, X-Ray Spectrom. **33**, 256 (2004).

[31] The transmission function determined from particle tracking simulations [11] (with the only input variable: the precisely known electromagnetic field of aSPECT) agrees with the analytical description of the spectrometer properties, i.e., protons move adiabatically through the MAC-E filter.

[32] F. Glück, Phys. Rev. D **47**, 2840 (1993).

[33] F. Glück, J. High Energy Phys. 09 (2023) 188.

[34] In contrast to [32], the relative radiative correction r_p [33] to the proton energy spectrum contains additional decimal places that have no effect on the measurement accuracy of a achieved [11].

[35] D. H. Wilkinson, Nucl. Phys. **A377**, 474 (1982) and references therein.

[36] S. Weinberg, Phys. Rev. **115**, 481 (1959).

[37] F. Glück, I. Joo, and J. Last, Nucl. Phys. **A593**, 125 (1995).

[38] In complete agreement with Eqs. (9)–(15) of Ref. [12].

[39] J. Beringer *et al.* (Particle Data Group), Phys. Rev. D **86**, 010001 (2012).

[40] R. L. Workman *et al.* (Particle Data Group), Prog. Theor. Exp. Phys. **2022**, 083C01 (2022) and 2023 update.

[41] H. Saul, C. Roick, H. Abele, H. Mest, M. Klopf, A. K. Petukhov, T. Soldner, X. Wang, D. Werder, and B. Märkisch, Phys. Rev. Lett. **125**, 112501 (2020).

[42] K. P. Hickerson *et al.* (UCNA Collaboration), Phys. Rev. C **96**, 042501(R) (2017).

[43] X. Sun *et al.*, Phys. Rev. C **101**, 035503 (2020).

[44] M. T. Hassan *et al.*, Phys. Rev. C **103**, 045502 (2021).

[45] F. E. Wietfeldt *et al.*, arXiv:2306.15042v1.

[46] D. Mund, B. Märkisch, M. Deissenroth, J. Krempel, M. Schumann, H. Abele, A. K. Petukhov, and T. Soldner, Phys. Rev. Lett. **110,** 172502 (2013).

[47] O. Erten and C. V. Deutsch, Combination of multivariate Gaussian distributions through error ellipses, *Geostatistics Lessons*, edited by J. L. Deutsch (2020), http://geostatisticslessons.com/lessons/errorellipses.

[48] N. Orsini, R. Bellocco, and S. Greenland, Stata J. **6,** 40 (2006).

[49] N. M. Blachman, IEEE Trans. Aerosp. Electron. Syst. **25,** 284 (1989).

[50] M. Bychkov et al., Phys. Rev. Lett. **103,** 051802 (2009).

[51] T. Bhattacharya, V. Cirigliano, S. D. Cohen, A. Filipuzzi, M. González-Alonso, M. L. Graesser, R. Gupta, and H.-W. Lin, Phys. Rev. D **85,** 054512 (2012).

[52] V. Cirigliano, D. Díaz-Calderón, A. Falkowski, M. González-Alonso, and A. Rodríguez-Sánchez, J. High Energy Phys. 04 (2022) 152.

[53] A. Falkowski, M. González-Alonso, and O. Naviliat-Cuncic, J. High Energy Phys. 04 (2021) 126.

[54] J. C. Hardy and I. S. Towner, Phys. Rev. C **91,** 025501 (2015).

[55] R. Gupta, Y.-C. Jang, B. Yoon, H.-W. Lin, V. Cirigliano, and T. Bhattacharya, Phys. Rev. D **98,** 034503 (2018).

[56] A. Czarnecki, W. J. Marciano, and A. Sirlin, Phys. Rev. D **100,** 073008 (2019).

[57] For $|V_{ud}|$ we took the PDG value [40].

[58] A. N. Ivanov, R. Höllwieser, N. I. Troitskaya, M. Wellenzahn, and Ya. A. Berdnikov, Phys. Rev. C **98,** 035503 (2018).

[59] M. T. Burkey et al., Phys. Rev. Lett. **128,** 202502 (2022).

[60] V. Cirigliano, M. González-Alonso, and M. L. Graesser, J. High Energy Phys. 02 (2013) 046.

[61] J. Fry et al., EPJ Web Conf. **219,** 04002 (2019).

[62] D. Dubbers, H. Abele, S. Baeßler, B. Märkisch, M. Schumann, T. Soldner, and O. Zimmer, Nucl. Instrum. Methods Phys. Res., Sect. A **596,** 238 (2008).

[63] G. Konrad et al. (PERC Collaboration), J. Phys. **340,** 012048 (2012).